Experimental and Computational Studies of $R_3Al-ER'_3$ (E = P, As, Sb, Bi; R = Et, *t*-Bu; R′ = $SiMe_3$, *i*-Pr) Donor−Acceptor Complexes: Role of the Central Pnictine and the Substituents on the Structure and Stability of Alane Adducts

Andreas Kuczkowski,[†] Stephan Schulz,*[,†] Martin Nieger,[†] and Peter R. Schreiner*[,‡]

Institut für Anorganische Chemie der Universität Bonn, Gerhard-Domagk-Strasse 1, D-53121 Bonn, Germany, and Department of Chemistry, University of Georgia, 510 Chemistry Building, Athens, Georgia 30602-2556

Received January 9, 2002

Donor−acceptor interactions within analogously substituted Lewis acid−base adducts of the type $Et_3Al-E(SiMe_3)_3$ and *t*-$Bu_3Al-E(i\text{-}Pr)_3$ (E = P, As, Sb, Bi) were investigated in the solid state, on the basis of single-crystal X-ray structure analyses, and in solution by temperature-dependent NMR spectroscopy. In addition, density functional theory computations (B3LYP/SDD) were performed to analyze molecular structures and to derive dissociation energies (D_e) of the $R_3Al-ER'_3$ adducts. The thermodynamic stability of these depends both on the electronic strength of the Lewis acid and base, which is influenced by the central group 13 and 15 elements and their substituents R and R′, and on steric interactions between the Lewis acid and base. Such repulsive interactions are decisive for the stability of adducts containing small central elements such as P and large substituents such as *i*-Pr and *t*-Bu. Comparisons between central structure parameters (Al−E and Al−C(H) bond distances; C(H)−Al−C(H) bond angles) and D_e values of several adducts show that the Al−E bond length does not necessarily display the thermodynamic stability of an adduct, while the Al−C(H) bond distance and C(H)−Al−C(H) bond angles are useful structural parameters to estimate the stability of an adduct in the solid state.

Introduction

Lewis acid−base reactions between group 13 (R_3M) and group 15 compounds (R_3E) have been widely studied for more than two centuries,[1] due both to their fascinating structural chemistry and to their importance in organic as well as inorganic synthesis. More recently, their potential use as single-source precursors for the preparation of binary materials have rendered them very attractive for materials scientists. In particular borane, alane, and gallane adducts with amines as well as phosphines of the type H_3M-ER_3 (M = B, Al, Ga; E = N, P) were synthesized and structurally characterized;[2] their dissociation enthalpies were determined experimentally. Fundamental theoretical investigations of group 13 trihalides and trihydrides MX_3 (X = F, Cl, Br, I, H) and group 15 trihydrides EH_3 were performed in the past decade.[3] The role of the central atoms M and E as well as the influence on the adduct stability of different substituents bound to the central elements, i.e., their dissociation energies, were studied.[4]

In contrast, adducts of the heavier group 15 elements, stibines R_3Sb[5] as well as bismuthines R_3Bi, have scarcely been synthesized and, as a consequence, structural as well as thermodynamic data such as dissociation energies are virtually unavailable. To the best of our knowledge, only Coates examined the thermodynamic stability of these types of adducts.[6] He investigated reactions of $GaMe_3$ with trimethylpnictines EMe_3 (E = N, P, As, Sb, Bi), leading partly to the formation of the expected $Me_3Ga-EMe_3$ adducts (E = N, P, As, Sb), except for $BiMe_3$, which did not form a stable compound. The gas-phase dissociation energies steadily decrease from the amine to the stibine adducts. In fact,

* To whom correspondence should be addressed. Fax: S.S., (Int) + 228 73-5327; P.R.S., (Int) + 706 542−9454. E-mail: S.S., sschulz@uni-bonn.de; P.R.S., prs@chem.uga.edu.
[†] Institut für Anorganische Chemie der Universität Bonn.
[‡] University of Georgia.

(1) The first reaction of this type was investigated by Gay−Lussac almost 200 years ago, who synthesized the first compound of this type, $F_3B{\cdot}NH_3$ (Gay-Lussac, J. L.; Thenard, J. L. *Mem. Phys. Chim. Soc. d'Arcueil* **1809**, *2*, 210. As cited in: Jonas, V.; Frenking, G. *J. Chem. Soc., Chem. Commun*. **1994**, 1489−1490.).

(2) For review articles see for example: (a) Jones, C.; Koutsantonis, G. A.; Raston, C. L. *Polyhedron* **1993**, *12*, 1829. (b) Gardiner, M. G.; Raston, C. L. *Coord. Chem. Rev*. **1997**, *166*, 1.

(3) See the following and the references therein: (a) Haaland, A. *Angew. Chem., Int. Ed. Engl*. **1989**, *28*, 992. (b) Haaland, A. In *Coordination Chemistry of Aluminum*; Robinson, G. H., Ed.; VCH: Weinheim, Germany, 1993. (c) Brunel, J. M.; Faure, B.; Maffei, M. *Coord. Chem. Rev*. **1998**, *178−180*, 665. (d) Anane, H.; Jarid, A.; Boutalib, A. *J. Phys. Chem. A* **1999**, *103*, 9847. (e) Jarid, A.; Boutalib, A. *J. Phys. Chem. A* **2000**, *104*, 9220.

(4) (a) Jonas, V.; Frenking, G.; Reetz, M. T. *J. Am. Chem. Soc.* **1994**, *116*, 8741. (b) Timoshkin, A. Y.; Suvorov, A. V.; Bettinger, H. F.; Schaefer, H. F., III. *J. Am. Chem. Soc.* **1999**, *121*, 5687.

10.1021/om0200205 CCC: $22.00
Publication on Web 03/03/2002

$Me_3Ga-SbMe_3$ was too unstable under these conditions, so that the exact dissociation enthalpy could not be determined. The decreasing basicity with increasing atomic number of the central group 15 element, which corresponds to the increased s character of the *lone pair* of the heavier group 15 elements,[7] is now generally accepted.[8] To the best of our knowledge, theoretical calculations examining both the structures and the thermodynamic stabilities of stibine and bismuthine adducts have never been performed.

In an attempt to gain further insight into this essentially unexplored class of compounds, Wells et al. and we started initial experimental work about 4 years ago. While Wells has been focusing on gallane−stibine adducts, we have been concentrating our efforts on the synthesis of stable alane−stibine adducts. In some cases, their solid-state structures were determined by single-crystal X-ray diffraction studies.[9] More recently, the first alane− and gallane−bismuthine adducts were synthesized and structurally characterized.[10] We found that the central Al−E adduct bond lengths cannot be used to estimate the strength of the Lewis acid−base interactions. However, the relative stability of such adducts can be estimated by following a model described by Haaland.[3a,b]

Adduct formation leads to an *increase of the Al−C bond lengths* and a *decrease of the C−Al−C bond angles* compared to those of the uncomplexed trialkylalane (Figure 1). The longer the Al−C bond distance and the smaller the C−Al−C bond angle, the stronger the Lewis acid−base interactions. Comparison of the bond elongation and the bond angle decrease of different adducts containing the same Lewis acid (trialkylalane) and different Lewis bases may help quantify the adduct

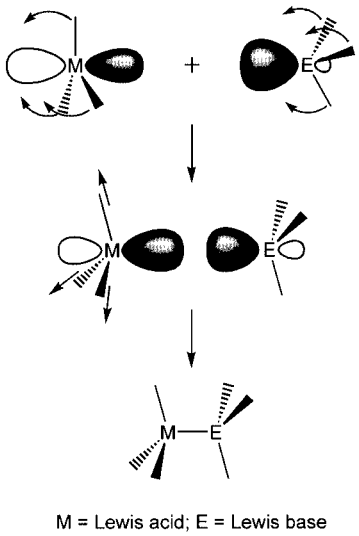

Figure 1. Changes of the structural parameters due to adduct formation according to the Haaland model.

strength and the influence of the Lewis basicity as well as steric interactions. These studies for several Al−Sb adducts[9d] led to the question if this model is useful for estimating adduct stabilities of a complete $R_3Al-ER'_3$ (E = P, As, Sb, Bi) family. However, no such group of adducts has been structurally characterized to date.

We have now synthesized adducts of the type $Et_3Al-E(SiMe_3)_3$ and $t\text{-}Bu_3Al-E(i\text{-}Pr)_3$ (E = P, As) and characterized them by single-crystal X-ray diffraction studies, allowing for the first time a systematic comparison of structural data of identically substituted adducts (E = P, As, Sb, Bi).[11] Since we were not only interested in their relative stabilities in the solid state, we also investigated $t\text{-}Bu_3Al-E(i\text{-}Pr)_3$ adducts in solution by temperature-dependent ^1H NMR spectroscopy.[12] In addition, both the structures and the dissociation enthalpies of several analogously substituted alane adducts were investigated in detail using density functional theory (DFT) methods in conjunction with effective core potentials. The influence of the central group 15 elements and the ligands on the adduct strength are presented.

Experimental Section

General Considerations. All manipulations were performed in a glovebox under an N_2 atmosphere or by standard Schlenk techniques. Et_3Al is commercially available from Aldrich and was used as received, while $t\text{-}Bu_3Al$,[13] $P(SiMe_3)_3$,[14] $As(SiMe_3)_3$,[14] $P(i\text{-}Pr)_3$,[15] and $As(i\text{-}Pr)_3$[16] were prepared by literature methods. ^1H, $^{13}C\{^1H\}$, and $^{31}P\{^1H\}$ NMR spectra

(5) Syntheses (no structural reports) of group 13−stibine adducts were reported by: (a) Hewitt, F.; Holliday, A. K. *J. Chem. Soc.* **1953**, 530. (b) Denniston, M. L.; Martin, D. R. *J. Inorg. Nucl. Chem.* **1974**, *36*, 2175. (c) Mente, D. C.; Mills, J. L.; Mitchell, R. E. *Inorg. Chem.* **1975**, *14*, 123. (d) Mente, D. C.; Mills, J. L. *Inorg. Chem.* **1975**, *14*, 1802. (e) Takashi, Y.; Aishima, I. *J. Organomet. Chem.* **1967**, *8*, 209. (f) Patterson, D. B.; Carnevale, A. *J. Chem. Phys.* **1973**, *59*, 6464. (g) Tsvetkov, V. G.; Kozyrkin, B. I.; Fukin, K. K.; Galiallina, R. F. *Zh. Obshch. Khim.* **1977**, *47*, 2155. (h) Gribov, B. G.; Kozyrkin, B. I.; Zorina, E. N. *Dokl. Akad. Nauk SSSR* **1972**, *204*, 350. (i) Zorina, E. N.; Gribov, B. G.; Kozyrkin, B. I.; Bogdanova, L. N. *Sb. Nauchn. Tr. Probl. Mikroelektron.* **1974**, *19*, 148; *Chem. Abstr.* **1975**, *83*, 1571347m. (j) Tsvetkov, V. G.; Novoselova, N. V.; Gribov, B. G. *Tr. Khim. Tekhnol.* **1972**, *65*; *Chem. Abstr.* **1973**, *79*, 77865z. (k) Whaley, T. P.; Norman, V. U.S. Patent 3,071,493, 1963; *Chem. Abstr.* **1963**, *58*, 4235.

(6) Coates, G. E. *J. Chem. Soc.* **1951**, 2003.

(7) However, detailed investigations show two significant steps within the decrease of the basicity: arsines AsR_3 exhibit a much lower basicity than phosphines PR_3 due to the post-transition-metal effect (*d contraction*), and bismuthines BiR_3 show a much lower basicity than stibines SbR_3 due both to the inert pair effect (*lanthanide contraction*) and to relativistic effects. See for example: Lange, K. C. H.; Klapötke, T. M. In *The Chemistry of Functional Groups: The Chemistry of Organic Arsenic, Antimony and Bismuth Compounds*; Wiley: New York, 1994; p 322 ff.

(8) Dissociation enthalpies for numerous compounds, in particular NH_3 and NMe_3 adducts, are available. See for example: Gur'yanova, E. N.; Gol'dshtein, I. P.; Romm, I. P. In *Donor−Acceptor Bond*; Wiley: New York, 1975.

(9) (a) Schulz, S.; Nieger, M. *J. Organomet. Chem.* **1998**, *570*, 275. (b) Schulz, S.; Nieger, M. *Organometallics* **1999**, *18*, 315. (c) Schulz, S.; Nieger, M. *J. Chem. Soc., Dalton Trans.* **2000**, 639. (d) Schulz, S.; Kuczkowski, A.; Nieger, M. *J. Organomet. Chem.* **2000**, *604*, 202. (e) Lube, M. S.; Wells, R. L.; White, P. S. *J. Chem. Soc., Dalton Trans.* **1997**, 285. (f) Baldwin, R. A.; Foos, E. E.; Wells, R. L.; White, P. S.; Rheingold, A. L.; Yap, G. P. A. *Organometallics* **1996**, *15*, 5035. (g) Wells, R. L.; Foos, E. E.; White, P. S.; Rheingold, A. L.; Liable-Sands, L. M. *Organometallics* **1997**, *16*, 4771.

(10) (a) Kuczkowski, A.; Thomas, F.; Schulz, S.; Nieger, M. *Organometallics* **2000**, *19*, 5758. (b) Kuczkowski, A.; Schulz, S.; Nieger, M. *Eur. J. Inorg. Chem.* **2001**, 2605.

(11) The corresponding stibine and bismuthine adducts have been prepared previously and are described elsewhere.[9]

(12) Experimental gas-phase data on the thermodynamic stability of these adducts were not available, due to the lack of the required equipment. $Et_3Al-E(SiMe_3)_3$ adducts were not investigated, since Et_3Al is dimeric in solution and, therefore, proton resonances of uncomplexed Et_3Al cannot be obtained. It was also found by low-temperature NMR spectroscopy that $Et_3Al-Bi(SiMe_3)_3$ is fully dissociated in solution.[9g]

(13) Lehmkuhl, H.; Olbrysch, O.; Nehl, H. *Liebigs Ann. Chem.* **1973**, 708.

(14) Hermann, W. A.; Brauer, G. *Synthetic Methods of Organometallic and Inorganic Chemistry (Hermann/Brauer)*; Thieme: Stuttgart, Germany, 1996; Vol. 3 (Phosphorus, Arsenic, Antimony and Bismuth).

(15) *Houben Weyl: Methoden der Organischen Chemie*, 4th ed.; Thieme Verlag: Stuttgart, Germany, 1963; Vol. XII/1 (Organophosphorus Compounds Part 1).

Table 1. Crystallographic Data and Measurements for $Et_3Al-E(SiMe_3)_3$ (E = P, 1; E = As, 2) and t-$Bu_3Al-E(i$-$Pr)_3$ (E = P, 3; E = As, 4)

	1	2	3	4
mol formula	$C_{15}H_{42}AlPSi_3$	$C_{15}H_{42}AlAsSi_3$	$C_{21}H_{48}AlP$	$C_{21}H_{48}AlAs$
fw	364.71	408.66	358.54	402.49
cryst syst	monoclinic	monoclinic	rhombohedral	monoclinic
space group	$P2_1/c$ (No. 14)	$P2_1/c$ (No. 14)	$R\bar{3}$ (No. 146)	$P2_1/c$ (No. 14)
a, Å	14.2312(8)	14.7368(8)	8.7449(3)	13.5925(5)
b, Å	9.7955(6)	9.7383(6)	8.7449(3)	8.8818(3)
c, Å	16.9969(9)	16.7783(9)	8.7449(3)	19.7649(5)
α, deg	90	90	105.075(2)	90
β, deg	93.834(4)	91.871(4)	105.075(2)	91.293(2)
γ, deg	90	90	105.075(2)	90
V, Å^3	2364.1(2)	2406.6(2)	583.73(3)	2385.5(2)
Z	4	4	1	4
radiation (wavelength, Å)	Mo Kα (0.710 73)			
μ, mm^{-1}	0.299	1.592	0.156	1.462
temp. K	123(2)			
D_{calcd}, g cm^{-3}	1.025	1.128	1.020	1.121
cryst dimens (mm)	0.15 × 0.08 × 0.03	0.12 × 0.08 × 0.03	0.25 × 0.20 × 0.10	0.25 × 0.15 × 0.10
$2\theta_{max}$, deg	50.0	50.0	50.0	56.0
no. of rflns measd	19522	22356	5182	23773
no. of nonequiv rflns measd	4146	4203	1402	5748
R_{merge}	0.078	0.082	0.101	0.055
no. of params refined/restraints	181/0	181/0	70/1	208/0
R1,[a] wR2[b]	0.044, 0.107	0.045, 0.113	0.063, 0.137	0.025, 0.064
goodness of fit[c]	0.965	1.034	1.148	0.981
final max, min $\Delta\rho$, e Å^{-3}	0.315, −0.208	1.084, −0.373	0.412, −0.287	0.349, −0.515

[a] $R1 = \sum(||F_o| - |F_c||)/\sum|F_o|$ (for $I > 2\sigma(I)$). [b] $wR2 = \{\sum[w(F_o^2 - F_c^2)^2]/\sum[w(F_o^2)^2]\}^{1/2}$. [c] Goodness of fit $= \{\sum[w(|F_o^2| - |F_c^2|)^2]/(N_{observns} - N_{params})\}^{1/2}$.

were recorded using a Bruker AMX 300 spectrometer and are referenced to internal C_6D_5H ($\delta(^1H)$ 7.154, $\delta(^{13}C)$ 128.0) and external H_3PO_4, respectively. Melting points were measured in sealed capillaries and are not corrected. Elemental analyses were performed at the Mikroanalytisches Labor der Universität Bonn.

General Preparation of R_3Al-ER_3. Pure R_3Al (2 mmol) and R_3E (2 mmol) were combined in the glovebox. **1**−**4** immediately formed a white solid, which was dissolved in *n*-pentane (5 mL) and stored at −30 °C, resulting in the formation of colorless crystals in almost quantitative yield.

$Et_3Al-P(SiMe_3)_3$ (1). Mp: 178−180 °C. Anal. Found (calcd) for $C_{15}H_{42}AlPSi_3$ (M_r = 364.71): C, 48.87 (49.19); H, 11.33 (11.56). ^{1}H NMR (300 MHz, C_6D_5H, 25 °C): δ 0.23 (d, $^3J_{HP}$ = 4.8 Hz, 9 H, $SiMe_3$), 0.34 (q, $^3J_{HH}$ = 8.1 Hz, 2 H, MeCH_2Al), 1.45 (t, $^3J_{HH}$ = 8.1 Hz, 3 H, *Me*CH_2Al). $^{13}C\{^1H\}$ NMR (80 MHz, C_6D_5H, 25 °C): δ 1.7 (MeCH_2Al), 3.2 (d, $^2J_{PC}$ = 8.2 Hz, $SiMe_3$), 10.8 (*Me*CH_2Al). $^{31}P\{^1H\}$ NMR (300 MHz, *n*-pentane, 25 °C): δ −233.7.

$Et_3Al-As(SiMe_3)_3$ (2). Mp: 176 °C. Anal. Found (calcd) for $C_{15}H_{42}AlAsSi_3$ (M_r = 408.66): C, 43.68 (43.92); H, 10.12 (10.32). ^{1}H NMR (300 MHz, C_6D_5H, 25 °C): δ 0.29 (s, 9 H, $SiMe_3$), 0.34 (q, $^3J_{HH}$ = 8.3 Hz, 2 H, MeCH_2Al), 1.51 (t, $^3J_{HH}$ = 8.3 Hz, 3 H, *Me*CH_2Al). $^{13}C\{^1H\}$ NMR (80 MHz, C_6D_5H, 25 °C): δ 3.4 (MeCH_2Al), 3.8 ($SiMe_3$), 11.0 (*Me*CH_2Al).

(t-Bu)$_3$Al−P(i-Pr)$_3$ (3). Mp: 88−90 °C. Anal. Found (calcd) for $C_{21}H_{48}AlP$ (M_r = 358.54): C, 69.82 (70.34); H, 13.35 (13.49). ^{1}H NMR (300 MHz, C_6D_5H, 25 °C): δ 1.06 (dd, $^3J_{PH}$ = 11.8 Hz, $^3J_{HH}$ = 7.2 Hz, 6 H, Me_2CHP), 1.10 (s, 9 H, Me_3CAl), 1.72 (dsept, $^2J_{PH}$ = 2.8 Hz, $^3J_{HH}$ = 7.2 Hz, 1 H, Me$_2$*CH*P). $^{13}C\{^1H\}$ NMR (80 MHz, C_6D_5H, 25 °C): δ 21.1 (d, $^2J_{PC}$ = 12.2 Hz, Me_2-CHP), 22.3 (d, $^1J_{PC}$ = 16.0 Hz, Me$_2$*C*HP), 30.9 (Me_3CAl). $^{31}P\{^1H\}$ NMR (300 MHz, C_6D_5H, 25 °C): δ −18.2.

(t-Bu)$_3$Al−As(i-Pr)$_3$ (4). Mp: 69−71 °C. Anal. Found (calcd) for $C_{21}H_{48}AlAs$ (M_r = 402.44): C, 62.21 (62.66); H, 11.86 (12.02). ^{1}H NMR (300 MHz, C_6D_5H, 25 °C): δ 1.10 (s, 9 H, Me_3CAl), 1.13 (d, $^3J_{HH}$ = 7.2 Hz, 6 H, Me_2CHAs), 1.75 (sep, $^3J_{HH}$ = 7.4 Hz, 1 H, Me$_2$*CH*As). $^{13}C\{^1H\}$ NMR (80 MHz, C_6D_5H, 25 °C): δ 21.7 (Me_2CHAs), 23.1 (Me$_2$*C*HAs), 31.0 (Me_3CAl).

X-ray Structure Solution and Refinement. Crystallographic data of **1**−**4** are summarized in Table 1. Figures 2−5 show the ORTEP diagrams of the solid-state structures of **1**−**4**. Data were collected on a Nonius Kappa-CCD diffractometer. The structures of **1**, **3**, and **4** were solved by direct methods, and that of **2** was solved by Patterson methods (SHELXS-97);[17] all were refined by full-matrix least squares on F^2 (SHELXL-97).[18] All non-hydrogen atoms were refined anisotropically, and hydrogen atoms were refined by a riding model. Empirical absorption corrections were applied for **2** (minimum/maximum transmission 0.8384/0.9898) and **4** (minimum/maximum transmission 0.6781/0.8362).

Computational Methods

All computations were performed with Gaussian98[19] using Becke's three-parameter gradient-corrected exchange functional[20] and the Lee−Yang−Parr nonlocal correlation functional[21] (i.e., B3LYP). We utilized the Stuttgart−Dresden relativistic effective core potentials (SDD) for the As, Sb, and

(16) *Houben Weyl: Methoden der Organischen Chemie*, 4th ed.; Thieme Verlag: Stuttgart, Germany, 1963; Metalloorganic Complexes with Arsenic, Antimony, and Bismuth.

(17) Sheldrick, G. M. SHELXS-97, Program for Structure Solution. *Acta Crystallogr., Sect. A* **1990**, *46*, 467.

(18) Sheldrick, G. M. SHELXL-97, Program for Crystal Structure Refinement; Universität Göttingen, Göttingen, Germany, 1997.

(19) Frisch, M. J.; Trucks, G. W.; Schlegel, H. B.; Scuseria, G. E.; Robb, M. A.; Cheeseman, J. R.; Zakrzewski, V. G.; Montgomery, J. A., Jr.; Stratmann, R. E.; Burant, J. C.; Dapprich, S.; Millam, J. M.; Daniels, A. D.; Kudin, K. N.; Strain, M. C.; Farkas, O.; Tomasi, J.; Barone, V.; Cossi, M.; Cammi, R.; Mennucci, B.; Pomelli, C.; Adamo, C.; Clifford, S.; Ochterski, J.; Petersson, G. A.; Ayala, P. Y.; Cui, Q.; Morokuma, K.; Malick, D. K.; Rabuck, A. D.; Raghavachari, K.; Foresman, J. B.; Cioslowski, J.; Ortiz, J. V.; Stefanov, B. B.; Liu, G.; Liashenko, A.; Piskorz, P.; Komaromi, I.; Gomperts, R.; Martin, R. L.; Fox, D. J.; Keith, T.; Al-Laham, M. A.; Peng, C. Y.; Nanayakkara, A.; Gonzalez, C.; Challacombe, M.; Gill, P. M. W.; Johnson, B. G.; Chen, W.; Wong, M. W.; Andres, J. L.; Head-Gordon, M.; Replogle, E. S.; Pople, J. A. *Gaussian 98*, Rev. A9; Gaussian, Inc.: Pittsburgh, PA, 1998.

(20) Becke, A. D. *J. Chem. Phys.* **1993**, *98*, 5648−5652.

(21) (a) Lee, C.; Yang, W.; Parr, R. G. *Phys. Rev. B* **1988**, *37*, 785−789. (b) Miehlich, B.; Savin, A.; Stoll, H.; Preuss, H. *Chem. Phys. Lett.* **1989**, *157*, 200−216.

Bi atoms[22] and a standard double-ζ basis set for H, C, P, and Si.[23] This is currently the only feasible approach to treat such a large set of structures containing heavy atoms in a consistent fashion. A comparison of the computed and experimental structures for the $Et_3Al-M(SiMe_3)_3$ species shows that this formulation is quite acceptable for the geometries: the average error for the bond lengths is 4.5% and 1.7% for the bond angles. However, the calculated and experimental structure parameters for the alane fragment (Al−C bond distances; C−Al−C bond angles) within the sterically overcrowded $(t\text{-Bu})_3Al-E(i\text{-Pr})_3$ adducts differ more significantly, due to increased repulsive van der Waals interactions between the substituents.

The computed dissociation energies are systematically underestimated due to a lack of diffuse and polarization functions in the basis set and the incomplete inclusion of electron correlation (currently not feasible). However, the *trends* within the groups are reproduced very well. All optimized structures were characterized by frequency computations to identify them as minima (the number of imaginary frequencies, NIMAG, equals 0), unless noted otherwise. Symmetry constraints were only used when a minimum was found in a particular point group; otherwise, the structures were allowed to relax fully (C_1 point group). All absolute energies and zero-point vibrational energies (ZPVEs) are given in a table in the Supporting Information.

Results and Discussion

Synthesis. 1−4 were synthesized according to the method described for the synthesis of the corresponding stibine and bismuthine adducts. Combination of equimolar amounts of the alane and the respective phosphine and arsine immediately leads to the formation of colorless solids, which were recrystallized from *n*-pentane at −30 °C, giving in almost quantitative yield **1−4** in the form of colorless crystals. In comparison to the starting compounds, the proton resonances due to the organic ligands found in the adducts **1−4** are slightly shifted to lower (ligands bound to Al) and higher field strengths (ligands bound to P and As), respectively. The same tendency was observed for the corresponding stibine adducts, while the bismuthine adducts show almost the same chemical shifts as the free trialkyls, indicating extensive dissociation in solution. ^{31}P NMR spectra of **1** and **3** also show resonances shifted to higher field compared to the pure phosphines, as is typical for alane−phosphine adducts containing sterically bulky phosphines with increased donor ability.[24]

Single-Crystal X-ray Diffraction Studies (Figures 2−5 and Table 2). To probe the Haaland model,[3a,b] the structures of **1−4** in the solid state were studied by single-crystal X-ray diffraction. The corresponding stibine and bismuthine adducts have been reported previously.[9d,10b] Single crystals of **1−4** suitable for structure determination were grown from *n*-pentane at −30 °C.

In comparison to the sum of the covalent radii (Al−P = 2.350 Å and Al−As = 2.460 Å), the Al−P (2.555(2) Å, **1**; 2.667(2) Å, **3**) and Al−As bond lengths (2.654(2) Å, **2**; 2.839(1) Å, **4**) are significantly elongated. While those of **1** and **2** fall within typical ranges observed for dative

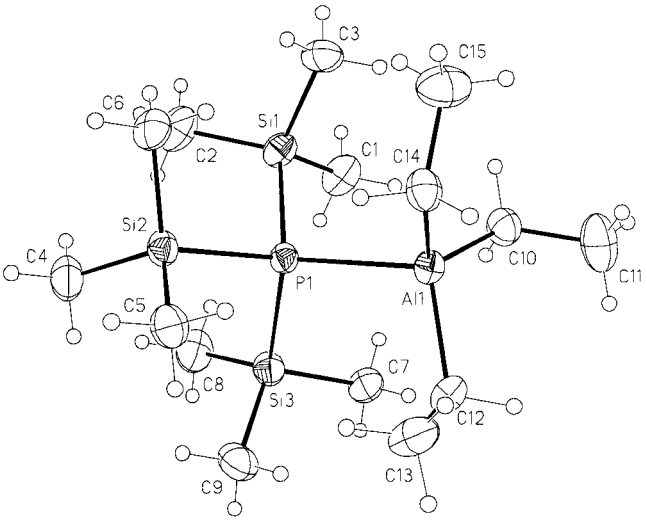

Figure 2. ORTEP plot (50% probability level) showing the solid-state structure and atom-numbering scheme for **1**.

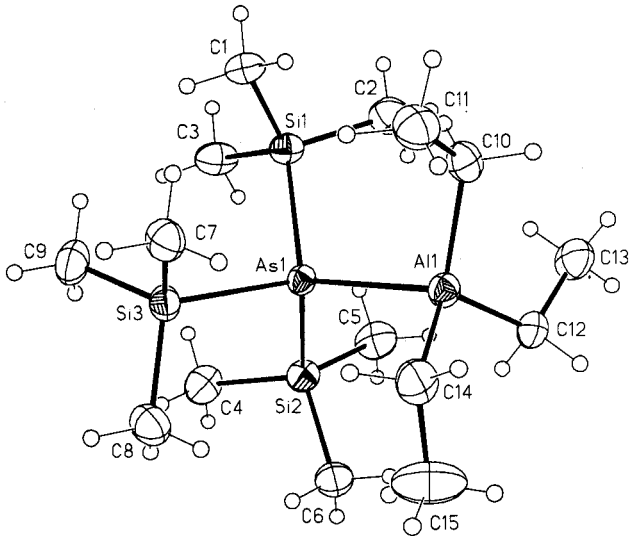

Figure 3. ORTEP plot (50% probability level) showing the solid-state structure and atom-numbering scheme for **2**.

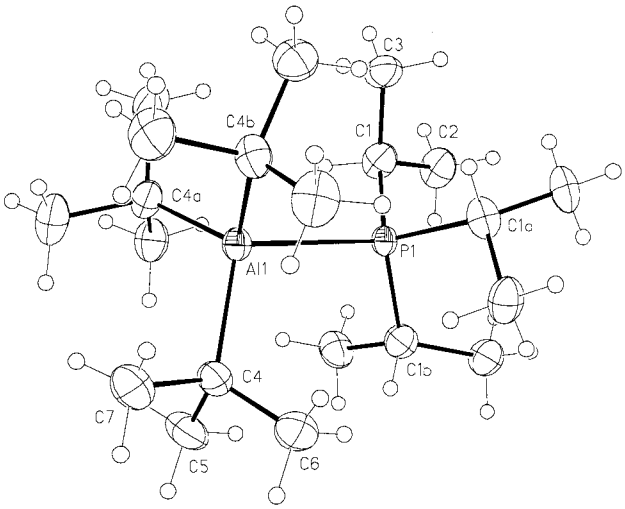

Figure 4. ORTEP plot (50% probability level) showing the solid-state structure and atom-numbering scheme for **3**.

Al−E bonds, $(t\text{-Bu})_3Al-E(i\text{-Pr})_3$ adducts **3** and **4** show extremely long bond distances. To the best of our knowledge, only $(neopentyl)_3Al-P(SiMe_3)_3$ (Al−P =

(22) (a) Andrae, D.; Häussermann, U.; Dolg, M.; Stoll, H.; Preuss, H. *Theor. Chim. Acta* **1990**, *77*, 123−141. (b) Bergner, A.; Dolg, M.; Küchle, W.; Stoll, H.; Preuss, H. *Mol. Phys.* **1993**, *80*, 1431−1441.

(23) (a) Dunning, T. H., Jr. *J. Chem. Phys.* **1970**, *53*, 2823−2833. (b) Dunning, T. H., Jr.; Hay, P. J. *Methods of Electronic Structure Theory*; Plenum Press: New York, 1977; Vol. 3.

(24) For a detailed study see for example: Barron, A. R. *J. Chem. Soc., Dalton Trans.* **1988**, 3047.

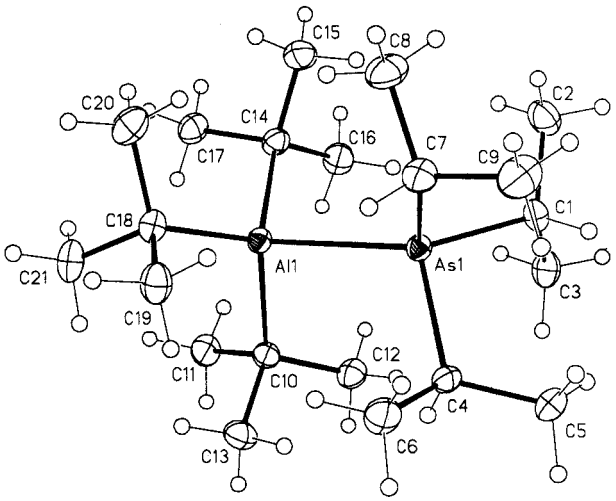

Figure 5. ORTEP plot (50% probability level) showing the solid-state structure and atom-numbering scheme for **4**.

Table 2. Bond Distances (Å) and Angles (deg) of 1−4 As Determined by Single-Crystal X-ray Diffraction

structure param	1	2	3	4
Al−E	2.555(2)	2.654(2)	2.667(2)	2.839(1)
Al−C	1.983(3)	1.981(4)	2.069(4)	2.034(2)
Al−C	1.992(3)	1.992(4)	2.069(4)	2.038(2)
Al−C	1.993(3)	1.993(4)	2.069(4)	2.048(2)
C−Al−C	116.9(2)	114.3(2)	112.6(2)	114.4(1)
C−Al−C	112.4(2)	113.9(2)	112.6(2)	113.8(1)
C−Al−C	111.4(2)	114.0(2)	112.6(2)	114.7(1)
C−Al−E	101.8(1)	106.0(2)	106.1(2)	106.3(1)
C−Al−E	106.8(1)	102.9(2)	106.1(2)	100.5(1)
C−Al−E	106.4(1)	104.2(2)	106.1(2)	105.4(1)
E−X	2.269(1)	2.362(2)	1.861(4)	1.991(2)
E−X	2.272(1)	2.366(2)	1.861(4)	1.994(2)
E−X	2.277(1)	2.366(2)	1.861(4)	1.999(2)
X−E−X	107.6(1)	106.1(1)	107.4(2)	104.0(1)
X−E−X	106.0(1)	105.5(1)	107.4(2)	103.1(1)
X−E−X	106.3(1)	104.5(1)	107.4(2)	100.2(1)
X−E−Al	114.7(1)	113.5(1)	111.5(2)	115.2(1)
X−E−Al	109.7(1)	113.3(1)	111.5(2)	121.8(1)
X−E−Al	112.1(1)	113.2(1)	111.5(2)	110.2(1)

2.680 Å)[25] and oligomeric $[H_3Al-(i\text{-}Pr_2PCH_2CH_2P(i\text{-}Pr_2)-AlH_3]_n$ (Al−P = 2.709, 2.754 Å)[26] show longer Al−P distances. The longest Al−As bond distances so far observed in (neopentyl)$_3$Al−As(SiMe$_3$)$_3$ (Al−P = 2.757 Å)[25] is about 0.08 Å shorter than those found in **4**.

The differences between the Al−E bond lengths within the Et$_3$Al−E(SiMe$_3$)$_3$ adduct group (0.37 Å) and the (t-Bu)$_3$Al−P(i-Pr)$_3$ adduct group (0.42 Å) display almost exactly the increase of the sum of the covalent radii (0.40 Å). The relative adduct stabilities, which are expected to decrease with increasing atomic number of the pnictine, are not expressed by this central structural parameter. However, the elongation of the Al−E bond lengths within the (t-Bu)$_3$Al−P(i-Pr)$_3$ adduct group is not steady. Both the arsine (2.839 Å) and the bismuthine adduct (3.088 Å) show Al−E distances significantly longer than expected. Due to increased steric interactions, the bond lengths of (t-Bu)$_3$Al−E(i-Pr)$_3$ adducts are longer than those of the Et$_3$Al−E(SiMe$_3$)$_3$ adducts. In particular, the Al−As bond distance found in **4**, which is about 0.18 Å elongated compared to those of **2**, is unexpectedly long.

The Al−C bond distances and C−Al−C bond angles steadily decrease with increasing atomic number of the pnictine. While the shortening of the Al−C bond lengths observed for the Et$_3$Al−E(SiMe$_3$)$_3$ adducts is only marginal (from 1.989 to 1.978 Å), the distances observed in the (t-Bu)$_3$Al−E(i-Pr)$_3$ adducts differ by about 0.05 Å (from 2.069 to 2.019 Å). In contrast, the increase of the C−Al−C bond angle sum found in both adduct groups is similar. The Et$_3$Al−E(SiMe$_3$)$_3$ adducts show an increase of about 10° and the (t-Bu)$_3$Al−P(i-Pr)$_3$ adducts of 13°. According to the Haaland model, both the smaller elongation of the Al−C bond lengths and the wider C−Al−C bond angles with increasing atomic number of the pnictines point to a decrease of the adduct stability. Even if the differences are small, in particular for the Et$_3$Al−E(SiMe$_3$)$_3$ adducts, the trends observed meet exactly the expectations.

NMR Studies (Figure 6 and Table 3). To obtain reliable thermodynamic data on the adducts in solution, temperature-dependent ^{1}H NMR studies were performed. The dissociation enthalpy of the adducts t-Bu$_3$Al−E(i-Pr)$_3$ can be derived from the temperature dependence of the equilibrium constant K_{eq}, with

$$t\text{-Bu}_3\text{Al} + \text{E}(i\text{-Pr})_3 \overset{K_{eq}}{\rightleftharpoons} \text{t-Bu}_3\text{Al}-\text{E}(i\text{-Pr})_3 \qquad (1)$$

and

$$\ln K_{eq} = \frac{-\Delta H_D}{R}\left(\frac{1}{T}\right) + \frac{\Delta S_D}{R} \qquad (2)$$

The equilibrium constant can be expressed in terms of the mole fraction of the alane present as free t-Bu$_3$Al and the total initial concentration, [total]:

$$K_{eq} = \frac{[\text{total}](\chi_{free})^2}{(1-\chi_{free})} \qquad (3)$$

Since the time-dependent ^{1}H NMR spectra only show one single resonance due to the Al−(t-Bu) group over the complete temperature range, and assuming the ^{1}H NMR shift of the Al−(t-Bu) group to be directly proportional to the mole fraction of the total species present as free t-Bu$_3$Al, χ_{free} may be calculated from the ^{1}H NMR chemical shift of Al−(t-Bu) at a given temperature:

$$\chi_{free} = \frac{\delta_{sample} - \delta_{coord}}{\delta_{free} - \delta_{coord}} \qquad (4)$$

δ_{free} is the chemical shift of the uncomplexed t-Bu$_3$Al, and δ_{sample} is obtained directly from the sample. δ_{coord} displays the "real" chemical shift of the adduct (fully coordinated species), which was estimated by addition of a 5-fold excess of the corresponding pnictine E(i-Pr)$_3$ to t-Bu$_3$Al, which was then measured at −70 °C, assuming t-Bu$_3$Al to be fully coordinated under these conditions.[27]

The dissociation enthalpies of **3**, **4**, and t-Bu$_3$Al−Sb(i-Pr)$_3$ were calculated as 12.2, 9.9, and 7.8 kcal/mol,

(25) Wells, R. L.; Foos, E. E.; Rheingold, A. L.; Yap, G. P. A.; Liable-Sands, L. M.; White, P. S. *Organometallics* **1998**, *17*, 2869.

(26) Bennett, F. R.; Elms, F. M.; Gardiner, M. G.; Koutsantonis, G. A.; Raston, C. L.; Roberts, N. K. *Organometallics* **1992**, *11*, 1497.

(27) Power, M. B.; Nash, J. R.; Healy, M. D.; Barron, A. R. *Organometallics* **1992**, *11*, 1830.

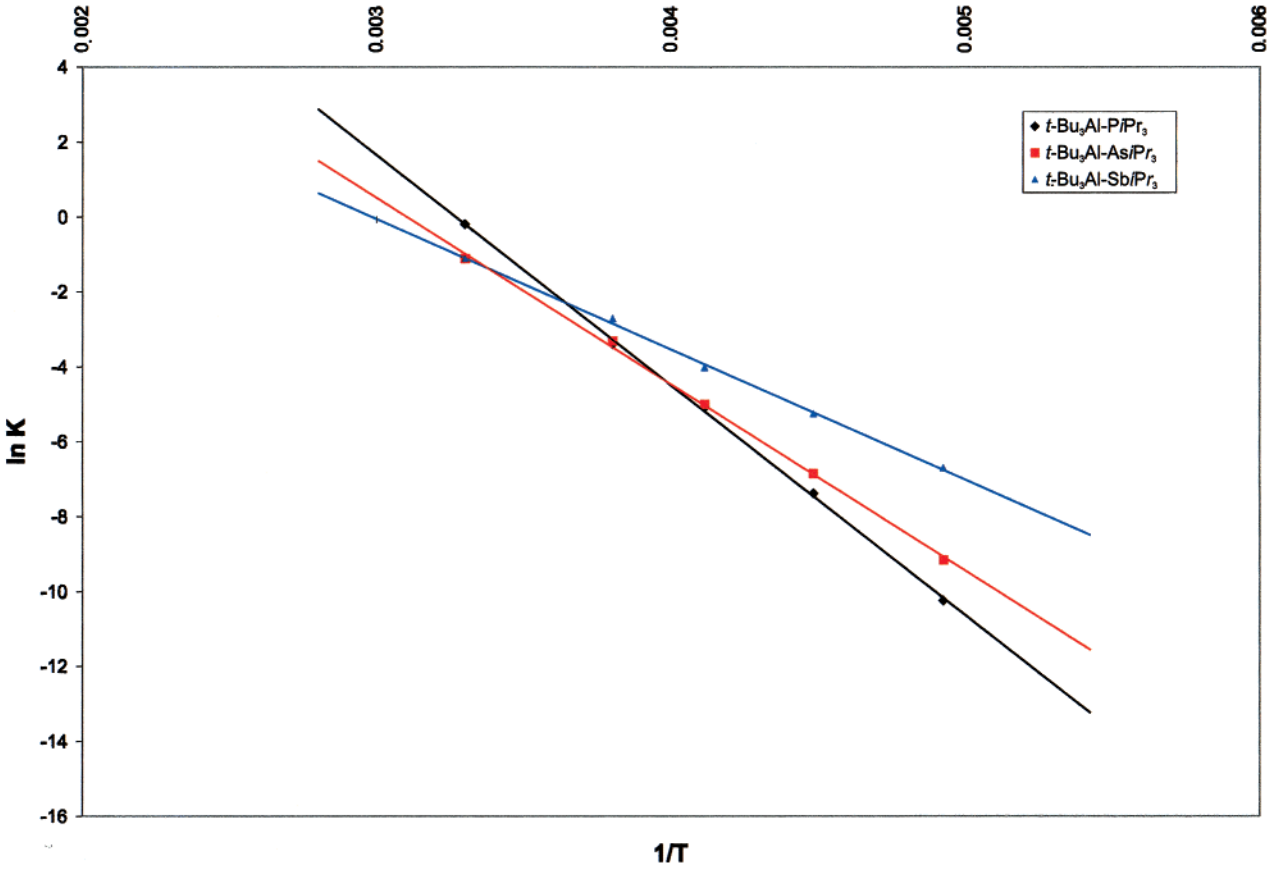

Figure 6. Temperature dependence of the equilibrium constant K_{eq} for the dissociation of **3** (R = 0.999), **4** (R = 0.998) and **5** (R = 0.997).

while the dissociation enthalpy of t-$Bu_3Al-Bi(i\text{-}Pr)_3$ is 6.9 kcal/mol.[9] Even if the absolute values are erroneous due to several potential sources of errors, in particular the chemical shifts of the "real" adducts,[28] the trend observed within this adduct group seems reasonable. The interaction between t-Bu_3Al and the pnictine i-Pr_3E in solution obviously becomes weaker with increasing atomic number of the pnictine. Since steric interactions become less important with increasing atomic radii of the central pnictine, the observed decreasing stability mostly results from the decreased Lewis basicity of the heavier pnictines.

Computational Studies. A detailed computational analysis was undertaken to gain deeper insights into the coordination properties of various triorganopnictines with different alanes. The results obtained clearly show the influence of basicity, acidity, and steric repulsion between the substituents on both the structural parameters and the thermodynamic adduct stability.

Free Donor and Acceptor Molecules. Experimentally (whenever available) and theoretically determined geometrical parameters of the donor and acceptor molecules are presented in Table 4. The theoretical and experimental geometries are in good agreement. The M−X (M = Al, E; X = H, C) distances are longer than experimentally determined, while there is no trend for the X−M−X bond angles.

$R_3Al-ER'_3$ (R, R′ = Alkyl) Adducts. The adducts typically have C_{3v} symmetry (exceptions are noted), with the substituents adopting a staggered orientation in relation to one another (Figure 7). Similar results were obtained by Timoshkin et al.[4b]

The largest structures in this series (t-$Bu_3Al-E(i\text{-}Pr)_3$ adducts) are very difficult to optimize, due to the rotational flexibility of the alkyl ligands. Moreover, the H···H repulsion of the alkyl groups becomes very important, so that the isopropyl groups on E have to point away from the Al−E bond to minimize to the lowest-lying structure. Nevertheless, some Al−E bond lengths are significantly overestimated due to the limitations in the basis set, which should include a number of diffuse functions to account properly for the underestimated dipolar long-range interactions (Table 5). Also, these types of complexes are challenging for DFT, because of the neglect of van der Waals terms in the current formulation of the functionals. While these deficiencies are recognized, there is little one can do for these types of structures at the moment due to their inherent flexibility. Needless to say, the methyl group rotations are accompanied by extremely flat potential

(28) A small variation of only 0.01 ppm would lead to ΔH values which would differ by about ±0.7 kcal/mol.
(29) Lide, D. R. In Handbook of Chemistry and Physics, 78th ed.; CRC Press: Boca Raton, FL, 1997; Table 9-15 ff.
(30) Rankin, D. W. H. Personal communication.
(31) Bruckmann, J.; Krüger, C. *Acta Crystallogr., Sect. C* **1995**, *C51*, 1155.
(32) Bruckmann, J.; Krüger, C. *Acta Crystallogr., Sect. C* **1996**, *C52*, 1733.
(33) Forsyth, G. A.; Rankin, D. W. H.; Robertson, H. E. *J. Mol. Struct.* **1990**, *239*, 209.
(34) Bruckmann, J.; Krüger, C. *Acta Crystallogr., Sect. C* **1995**, *C51*, 1152.
(35) Beagley, B.; Medwid, A. R. *J. Mol. Struct.* **1977**, *38*, 229.
(36) Breunig, H. J.; Jönsson, M.; Rosler, R.; Lork, E. *J. Organomet. Chem.* **2000**, *608*, 60.

Table 3. Temperature-Dependent ^{1}H NMR Chemical Shift and Thermodynamic Data of the *t*-Bu$_3$Al−E(*i*-Pr)$_3$ Adducts (E = P, As, Sb) in Toluene-d_8

t-Bu$_3$Al−P(*i*-Pr)$_3$ (**3**)

T [K]	$1/T$ (10^{-3} K^{-1})	δ_{exptl} (ppm)[a]	χ_{free}	K_{eq}	ln K
303	3.30	1.20	0.956	8.28×10^{-1}	−0.19
263	3.80	1.32	0.588	3.36×10^{-2}	−3.39
243	4.12	1.41	0.324	6.19×10^{-3}	−5.08
223	4.48	1.48	0.118	6.27×10^{-4}	−7.37
203	4.93	1.51	0.029	3.57×10^{-5}	−10.24

δ_{coord} (ppm)	δ_{free} (ppm)	concen	ΔH (kcal/mol)	ΔS (cal/(K mol))
1.52	1.18	0.04	12.2	39.8

t-Bu$_3$Al−As(*i*-Pr)$_3$ (**4**)

T [K]	$1/T$ (10^{-3} K^{-1})	δ_{exptl} (ppm)[a]	χ_{free}	K_{eq}	ln K
303	3.30	1.21	0.900	3.24×10^{-1}	−1.13
263	3.80	1.30	0.600	3.60×10^{-2}	−3.32
243	4.12	1.38	0.333	6.67×10^{-3}	−5.01
223	4.48	1.44	0.150	1.06×10^{-3}	−6.85
203	4.93	1.47	0.050	1.05×10^{-4}	−9.16

δ_{coord} (ppm)	δ_{free} (ppm)	concn	ΔH (kcal/mol)	ΔS (cal/(K mol))
1.48	1.18	0.04	9.9	30.6

t-Bu$_3$Al−Sb(*i*-Pr)$_3$

T [K]	$1/T$ (10^{-3} K^{-1})	δ_{exptl} (ppm)[a]	χ_{free}	K_{eq}	ln K
303	3.30	1.31	0.569	5.26×10^{-2}	−2.95
263	3.80	1.39	0.279	7.58×10^{-3}	−4.88
243	4.12	1.42	0.172	2.51×10^{-3}	−5.99
223	4.48	1.45	0.086	5.69×10^{-4}	−7.47
203	4.93	1.46	0.034	8.62×10^{-5}	−9.36

δ_{coord} (ppm)	δ_{free} (ppm)	concn	ΔH (kcal/mol)	ΔS (cal/(K mol))
1.47	1.18	0.07	7.8	20.0

[a] β-H resonance of *t*-Bu$_3$Al.

energy hypersurfaces, making all optimizations enormously time-consuming. This problem would only be amplified if the basis sets were extended. However, as the errors are systematic, the trend within the group of different E is, at least for the most part, preserved.

The calculated dissociation energies within analogously substituted adduct groups generally decrease with increasing atomic number of the pnictine, except for the *t*-Bu$_3$Al−E(*i*-Pr)$_3$ adducts (Figure 8). In this particular group the phosphine adduct is even less stable than the bismuthine adduct, while both the arsine and stibine adducts are the most stable in this series. This tendency is due to repulsive van der Waals interactions between the large *t*-Bu and *i*-Pr substituents, which become less important with increasing atomic radius of the central pnictines. Such interactions are obviously able to overcompensate attractive dipolar interactions between the alane and the Lewis base, leading in the case of *t*-Bu$_3$Al−P(*i*-Pr)$_3$ to a weaker adduct, despite the use of an electronically stronger Lewis base.

The D_e values obtained for the Me$_3$Al− and *t*-Bu$_3$Al− trialkylpnictine adducts typically range from 14 kcal mol^{-1} (Al−P adducts) to 3 kcal mol^{-1} (Al−Bi adducts), while the AlH$_3$ adducts are significantly more stable (22 kcal mol^{-1} (Al−P), 10 kcal mol^{-1} (Al−Bi)). Within each adduct group, the EH$_3$ adducts consistently show the lowest dissociation energies, except for the *t*-Bu$_3$Al phosphine and arsine adducts; within these specific groups, the E(*i*-Pr)$_3$ adducts are less stable than the EH$_3$ adducts due to steric repulsion between the substituents. The computational findings meet the expectations with respect to the different acceptor and donor properties of the Lewis acids and bases, due to different electron-withdrawing and electron-donating properties of the substituents. They also confirm the results obtained by Coates in his initial studies.

The dissociation energies within the H$_3$Al−ER′$_3$ (R′ = H, Et, *i*-Pr) and Me$_3$Al−ER′$_3$ (R′ = H, Me, Et, *i*-Pr) adduct families containing a constant Lewis acid AlR$_3$ but different substituted Lewis bases ER′$_3$ increase with increasing basicity of the pnictine, clearly showing the influence of the substituents bound to the Lewis base (Figure 9). However, such substituent effects on the

Table 4. B3LYP/SDD Optimized Structural Parameters for R$_3$Al and ER′$_3$ Compounds[a]

species	Al−C(H) (Å)	C−Al−C (deg)	E−C(H) (Å)	C−E−C (deg)
H$_3$Al	1.586[b]	120.0[b]		
Me$_3$Al	1.976 (1.957)[29]	120.0 (120.0)		
Et$_3$Al	1.987	120.0		
t-Bu$_3$Al	2.031 (2.004)[30]	119.8 (120.0)		
PH$_3$			1.443 (1.420)[29]	94.2 (93.3)
PMe$_3$			1.904 (1.847;[29,d] 1.833[31,e])	98.8 (98.6; 99.3)
PEt$_3$			1.917 (1.842[31,e])	98.7 (99.5)
P(*i*-Pr)$_3$			1.951 (1.863[32,e])	100.8 (103.2)
P(SiMe$_3$)$_3$			2.358[a] (2.259;[33,d] 2.245[34,e])	105.3[b] (105.1; 106.0)
AsH$_3$			1.539 (1.511)[29]	92.0 (92.1)
AsMe$_3$			2.004 (1.979)[29]	97.0 (98.8)
AsEt$_3$			2.014	96.9
As(*i*-Pr)$_3$			2.045	99.1
As(SiMe$_3$)$_3$			2.457[b]	102.2[b]
SbH$_3$			1.717 (1.704)[29]	91.2 (91.6)
SbH$_3$			2.184 (2.169)[35]	95.0 (94.2)
SbEt$_3$			2.197	94.5
Sb(*i*-Pr)$_3$			2.223	96.4
Sb(SiMe$_3$)$_3$			2.665[b] (2.564)[36,e]	98.8[b] (98.9)
BiH$_3$			1.815	90.8
BiMe$_3$			2.285 (2.263)[29]	94.4 (97.1)
BiEt$_3$			2.295	93.6
Bi(*i*-Pr)$_3$			2.316	95.7
Bi(SiMe$_3$)$_3$			2.722[b]	97.1[b]

[a] Experimental values (gas-phase data) are given in parentheses. [b] M−Si. [c] Averaged value. [d] Gas phase. [e] Solid state.

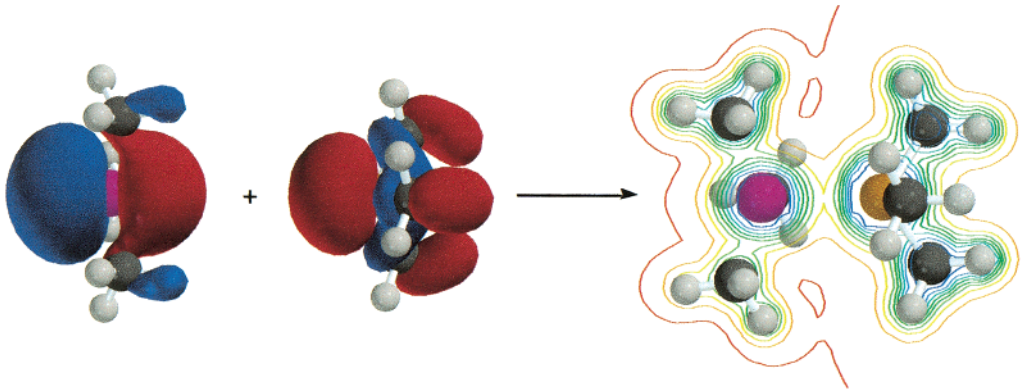

Figure 7. Generic orbital interactions of the studied adducts (left) and the electron density distribution in the plane containing the central metal atoms.

adduct stability are less important compared to the role of the central group 15 element. The basicity of Lewis bases ER'_3 increases according to the following sequence: R′ = H < Me < Et < *i*-Pr < *t*-Bu. Obviously, this is the result of both the constantly increasing steric demand of the substituents, leading to larger C−E−C bond angles and therefore reducing the s character of the lone pair, and the increasing electron donor properties (+I effect) of the substituents. In contrast, the *t*-Bu_3-Al−E(*i*-Pr)$_3$ adducts show no steady trend. The expected tendency is only observed for the bismuthine adducts, while the stability of the phosphine adducts decreases with increasing basicity of the phosphine. The D_e values of the arsine and stibine adducts, however, show a local maximum for the *t*-$Bu_3Al-EEt_3$ adducts, while the *t*-$Bu_3Al-E(i\text{-}Pr)_3$ adducts are less stable. These tendencies are due to repulsive interactions between the substituents, which are minimal in the case of the bismuthine adducts containing the largest group 15 element.

The decreasing Lewis acidity of the alanes according to the sequence $H_3Al > Me_3Al >$ *t*-Bu_3Al, resulting from the increased +I effect of the substituents, is expressed by the decreasing dissociation energies, as can clearly be seen within adducts of different alanes and a constant Lewis base ER'_3. In particular, the AlH_3 adducts are significantly more stable than the corresponding trialkylalane adducts.

Stabilities and Structural Parameters. According to the Haaland model, an increased thermodynamic stability of the adduct should be accompanied by a decrease of the average R−Al−R bond angle and an increase of the Al−R bond distance (R = H, Me, Et).[3a,b] The computed data strongly support these expectations. In all cases, a good correlation between the adduct stability as expressed by their D_e values and their central structure parameter (Al−C(H) bond length; C(H)−Al−C(H) bond angle) is found. However, comparisons should only be made for adducts containing the same Lewis acid, to eliminate any steric or electronic effects of the substituents bound to Al. In addition, the calculated data clearly demonstrate that Al−E bond distances are not useful for an estimation of the thermodynamic adduct stability, because thermodynamically more stable adducts do not necessarily exhibit shorter Al−E distances. In particular, the phosphine adducts (smallest group 15 element in our investiga-

Table 5. B3LYP/SDD Optimized Structural Parameters for $R_3Al-ER'_3$ Adducts[a]

E	Al−E (Å)	Al−C(H) (Å)	C−Al−C (deg)	E−C(H) (Å)	C−E−C (deg)	D_e (kcal/mol)	D_0 (kcal/mol)
			R = R′ = H				
P	2.654	1.595	118.7	1.425	98.8	13.5	10.9
As	2.765	1.593	119.0	1.518	96.4	9.5	7.2
Sb	3.049	1.592	119.3	1.698	94.9	6.4	4.5
Bi	3.174	1.590	119.7	1.799	93.4	2.9	1.3
			R = H; R′ = Et				
P	2.569	1.602	117.4	1.896	103.3	21.3	18.6
As	2.662	1.600	117.8	1.990	101.5	16.6	14.2
Sb	2.905	1.598	118.3	2.175	99.3	12.6	10.9
Bi	3.006	1.595	118.8	2.277	97.5	9.2	7.5
			R = H; R′ = *i*-Pr				
P	2.575	1.603	117.1	1.932	104.3	22.3	19.7
As	2.664	1.601	117.5	2.021	103.2	17.7	15.1
Sb	2.898	1.598	118.1	2.201	100.9	13.6	11.7
Bi	2.993	1.597	118.5	2.299	99.4	10.3	8.4
			R = Me; R′ = H				
P	2.791	1.988	118.5	1.429	97.6	7.4	5.5
As	2.985	1.983	119.0	1.525	94.8	4.3	2.8
Sb	3.453	1.961	119.4	1.707	93.0	2.0	0.9
Bi	3.822	1.977	120.0	1.809	91.5	0.4	−0.4
			R = Me; R′ = Me				
P	2.658	1.995	117.4	1.883	102.6	12.5	11.2
As	2.793	1.992	117.9	1.981	100.2	8.6	7.4
Sb	3.137	1.987	118.5	2.167	97.5	5.3	3.1
Bi	3.324	1.983	119.2	2.272	95.8	3.2	2.0
			R = Me; R′ = Et				
P	2.661	1.996	116.9	1.899	102.5	12.6	10.9
As	2.793	1.993	117.4[b]	1.994	100.3	8.8	7.4
Sb	3.116	1.989	118.3	2.184	97.6	5.7	4.3
Bi	3.284	1.984	119.0	2.283	95.8	3.6	2.6
			R = Me; R′ = *i*-Pr				
P	2.694	1.997	116.2[b]	1.931	100.7	13.6	12.0
As	2.838	1.993	116.9[b]	2.028	103.0	9.9	8.2
Sb	3.100	1.990	117.9[b]	2.207	99.4	6.7	5.4
Bi	3.248	1.986	118.8[b]	2.305	98.2	4.4	3.2
			R = *t*-Bu; R′ = H				
P	2.774	2.056	117.9	1.428	97.7	7.6	5.9
As	2.908	2.043	118.1	1.522	95.4	4.4	3.1
Sb	3.208	2.041	118.3	1.704	93.7	1.7	0.8
Bi	3.893	2.034	119.2	1.809	91.6	0.1	−0.5
			R = *t*-Bu; R′ = Et				
P	2.971	2.056	115.8	1.911	99.2	7.6	
As	3.097	2.049	116.8	2.004	97.4	6.4	
Sb	3.197	2.048	117.2[b]	2.185	96.5	5.8	
Bi	3.529	2.040	118.2[b]	2.289	94.2	2.6	

[a] D_e = dissociation energy at 0 K; $D_0 = D_e + \Delta ZPVE$. [b] C_1 structure: value averaged.

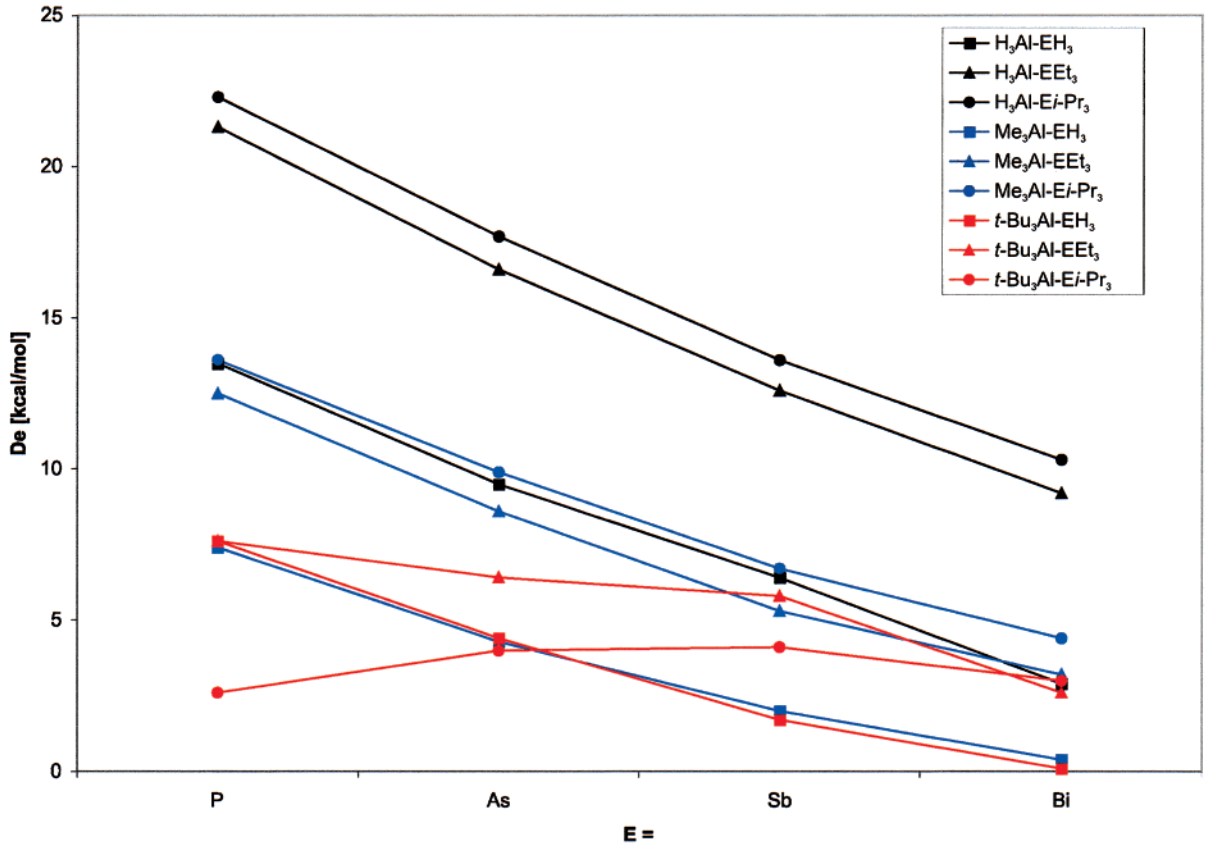

Figure 8. B3LYP/SDD optimized dissociation enthalpies D_e (kcal/mol) of $R_3Al-ER'_3$ adducts (R = H, Me, *t*-Bu; R′ = H, Et, *i*-Pr), showing the influence of the central pnictine on the adduct stability.

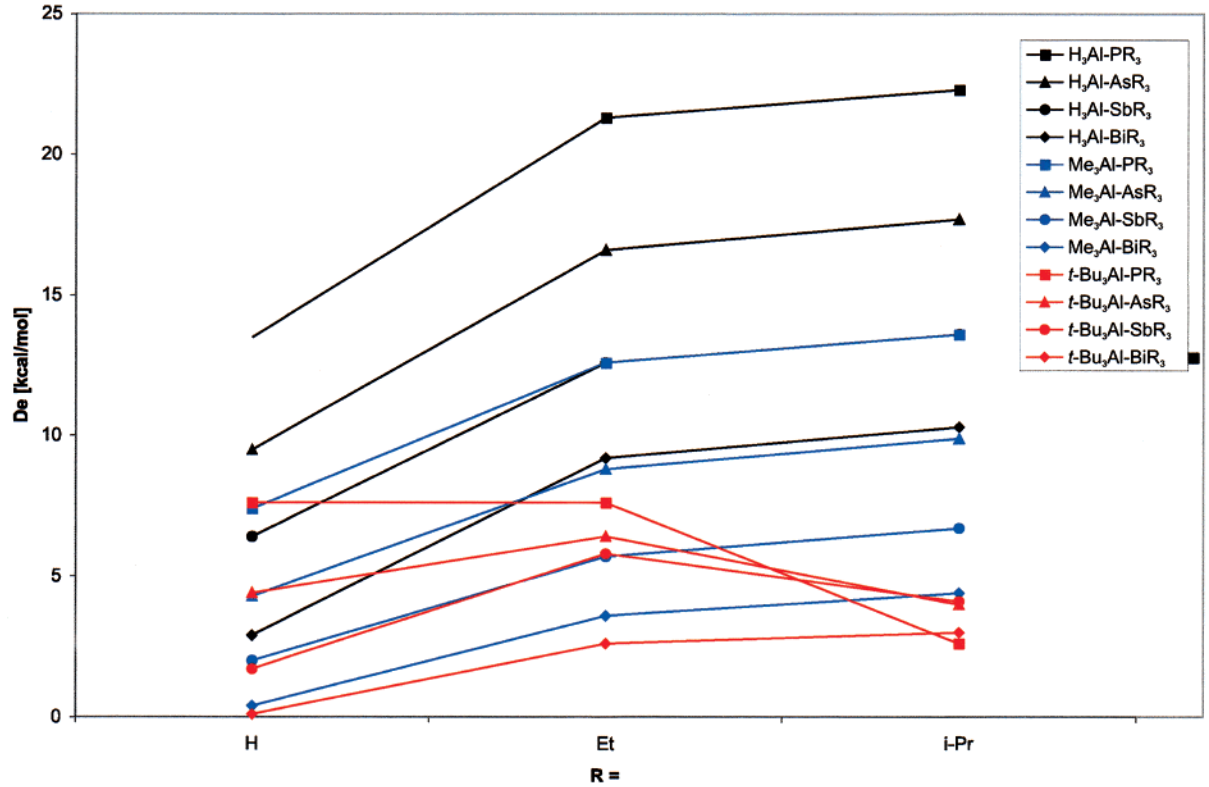

Figure 9. B3LYP/SDD optimized dissociation enthalpies D_e (kcal/mol) of $R_3Al-ER'_3$ adducts (R = H, Me, *t*-Bu; R′ = H, Et, *i*-Pr), showing the influence of the substituents bound to the pnictine on the adduct stability.

tions) as well as adducts containing large substituents (*t*-Bu_3Al) show no correlation between the thermodynamic stability and the Al−E bond distance. For these adducts repulsive steric interactions significantly influence the Al−E bond lengths. Nonbonding H···H distances between the methyl groups of *t*-Bu_3Al adducts

Table 6. B3LYP/SDD Optimized Structural Parameters (Averaged Values) for $Et_3Al-E(SiMe_3)_3$ and t-$Bu_3Al-E(i$-$Pr)_3$ Adducts[a]

E	Al−E (Å)	Al−C (Å)	C−Al−C (deg)	E−X (Å)	X−E−X (deg)	D_e (kcal/mol)	D_0 (kcal/mol)
			$Et_3Al-E(SiMe_3)_3$				
P	2.655 (2.555)	2.012 (1.989)	115.9 (113.6)	2.360	107.7	13.8	12.2
As	2.769 (2.654)	2.009 (1.989)	116.7 (114.1)	2.447	106.1	8.8	7.4
Sb	3.062 (2.841)	2.005 (1.984)	117.6 (115.8)	2.647	103.4	5.1	4.6
Bi	3.214 (2.921)	2.001 (1.978)	118.4 (116.9)	2.713	100.2	2.2	1.1
			t-$Bu_3Al-E(i$-$Pr)_3$				
P	3.378 (2.667)	2.050 (2.069)	116.5 (112.6)	1.937 (1.861)	106.5 (107.4)	2.6	
As	3.675 (2.839)	2.033 (2.040)	118.3 (114.3)	2.042 (1.995)	102.2 (102.4)	4.0	
Sb	3.532 (2.927)	2.042 (2.030)	117.6 (115.6)	2.218 (2.182)	96.3 (100.5)	4.1	
Bi	3.665 (3.088)	2.039 (2.019)	118.2 (116.8)	2.313 (2.295)	95.5 (95.5)	3.0	

[a] Experimental values are given in parentheses. D_e = dissociation energy at 0 K; $D_0 = D_e + \Delta ZPVE$.

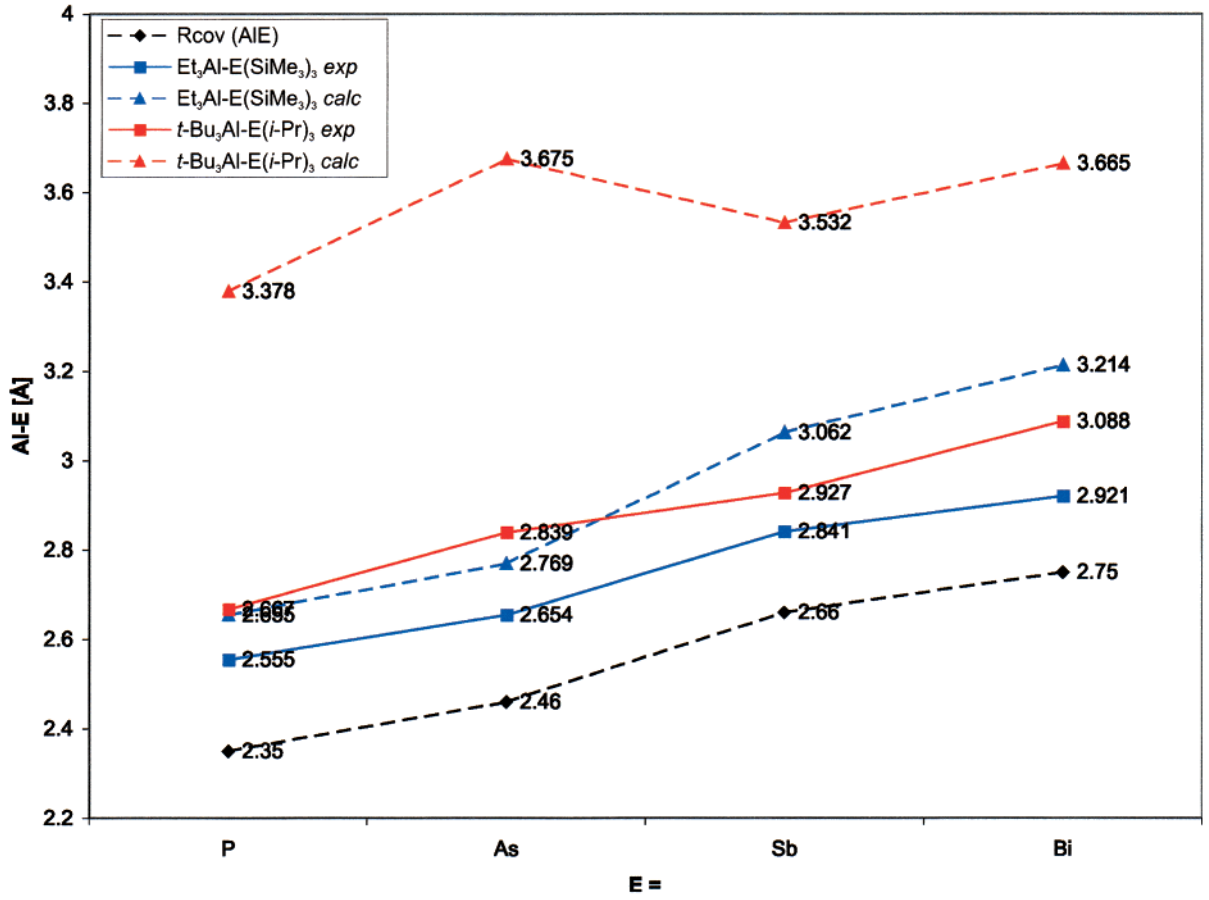

Figure 10. B3LYP/SDD optimized and experimental Al−E bond lengths (Å) of $Et_3Al-E(SiMe_3)_3$ and t-$Bu_3Al-E(i$-$Pr)_3$ adducts.

are <3 Å, indicative of repulsive interactions. The Al−E bond distances in the adducts display an equilibrium between Lewis acid−base strength (thermodynamic stability; the stronger the Lewis acid and/or base, the more stable the adduct and the shorter the Al−E bond length) and repulsive van der Waals interactions between the substituents (the larger the substituents, the longer the Al−E bond distance). The equilibrium position for adducts containing either small central atoms such as P or sterically demanding substituents (t-Bu, i-Pr) is mainly dominated by repulsive interactions, while thermodynamic stability plays the key role for adducts with small substituents (H, Me) and/or large central atoms such as Bi.

Comparison of Calculated and Experimental Data (Table 6 and Figures 10−12). Direct experimental gas-phase or solid-state structural data as well as thermodynamic data of the described adducts are essentially unknown. Only the t-$Bu_3Al-E(i$-$Pr)_3$ and $Et_3Al-E(SiMe_3)_3$ adducts, which have been completely structurally characterized by single-crystal X-ray diffraction, allow structural comparisons between the calculated and the experimentally obtained values.

$Et_3Al-E(SiMe_3)_3$. The calculated dissociation energies constantly decrease from $Et_3Al-P(SiMe_3)_3$ (D_e = 13.8 kcal mol^{-1}) to $Et_3Al-Bi(SiMe_3)_3$ (D_e = 2.2 kcal mol^{-1}). According to the Haaland model, the Al−C bond distances consequently decrease and the C−Al−C bond angles increase from the phosphine (Al−C = 2.012 Å; C−Al−C = 115.9°) to the bismuthine adduct (Al−C = 2.001 Å; C−Al−C = 118.4°). Those of pure Et_3Al are calculated as 1.987 Å and 120.0°. The computed bond distances and bond angles are only slightly larger than the experimentally determined values, with an average

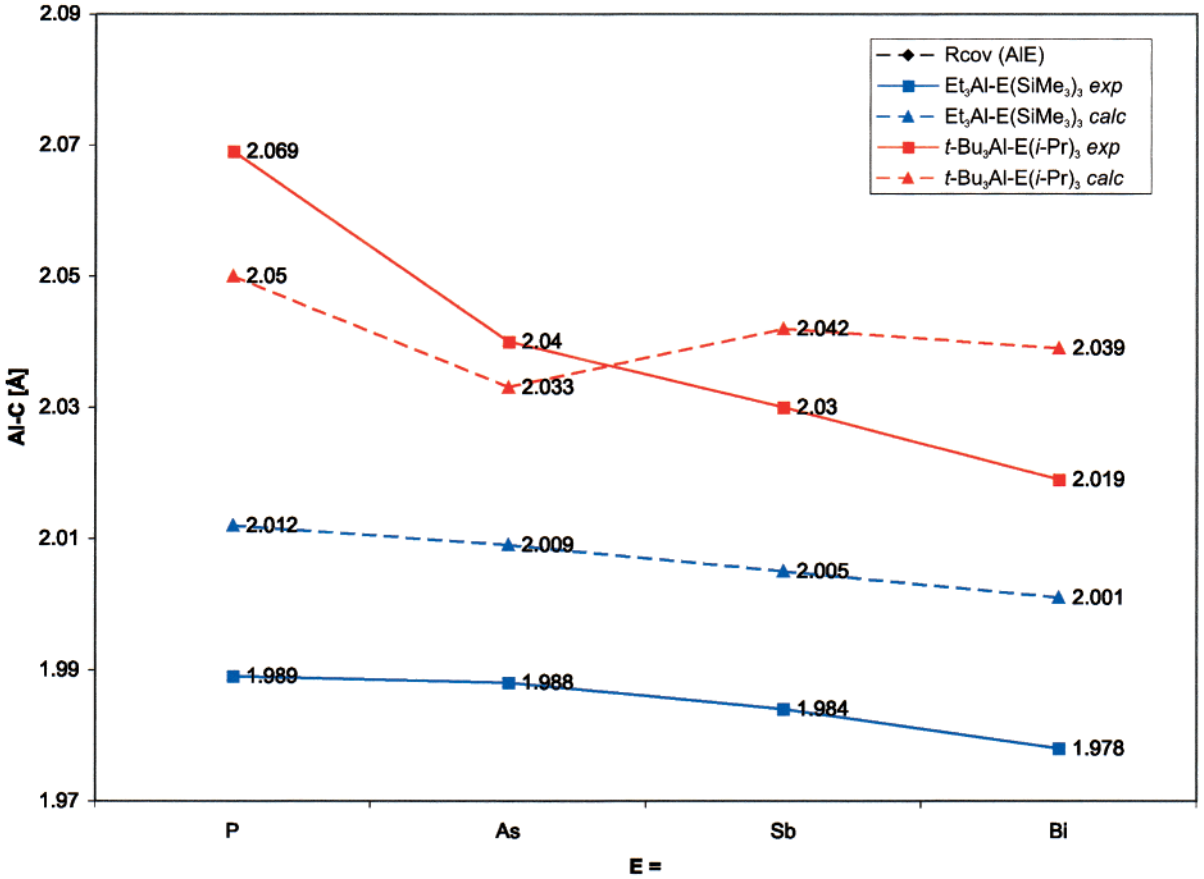

Figure 11. B3LYP/SDD optimized and experimental Al−C bond lengths (Å) of $Et_3Al-E(SiMe_3)_3$ and t-$Bu_3Al-E(i\text{-}Pr)_3$ adducts.

difference of 1% (Al−C) and 2% (C−Al−C), respectively. In contrast, the calculated and experimental M−E bond distances differ significantly. The data obtained from single-crystal X-ray structure analyses only show an increase of the Al−E bond length by 0.37 Å (Al−P = 2.555 Å; Al−As = 2.654 Å; Al−Sb = 2.841 Å; Al−Bi = 2.921 Å) according to the increase of the covalent radii of the group 15 elements (P, 1.10 Å; Bi, 1.50 Å), giving no indication for a decrease of the thermodynamic stability toward heavier group 15 element adducts. In contrast, the computed structures show a significant increase of the Al−E bond distances from 2.655 Å (Al−P) to 3.214 Å (Al−Bi). The computed and experimental values obtained for the stibine and bismuthine adducts differ by about 8 and 10%.

***t*-$Bu_3Al-E(i\text{-}Pr)_3$ Adducts.** The experimental structure data of the t-$Bu_3Al-E(i\text{-}Pr)_3$ adducts follow the same trends as were found for the $Et_3Al-E(SiMe_3)_3$ adducts. The Al−C bond lengths steadily decrease and the C−Al−C bond angles steadily increase with increasing atomic number of the pnictine, confirming the experimental findings for their dissociation energies as determined in solution by temperature-dependent NMR spectroscopy. The computed values for this particular adduct group do not exhibit this trend, since the values for the phosphine and arsine adducts do not display this tendency. The same is true for the calculated dissociation enthalpies D_e, which show a maximum for the arsine and stibine adducts. The phosphine adduct is significantly less stable, due to repulsive interactions between the bulky ligands. Such interactions are very important in the gas phase, which is also indicated by the problems occurring during the calculations, while they are less effective in solution and in the solid state. However, the trends observed for the computed Al−C and C−Al−C values agree with the trend observed for the thermodynamic stability of the adducts, demonstrating that the Haaland model is useful for the estimation of the relative stability within an adduct group. Experimentally observed and computed structural parameters show a good correlation with respect to the structural parameters of the Lewis base fragment, while the Al−C bond distances and C−Al−C bond angles differ significantly, in particular for the phosphine and arsine adducts. In addition, the Al−E bond lengths appear in the calculations far longer than experimentally observed. The differences are up to 0.73 Å for the arsine adduct t-$Bu_3Al-As(i\text{-}Pr)_3$.

Conclusions

For the first time the structures and thermodynamic stabilities of analogously substituted alane adducts, including those of stibines and bismuthines, were analyzed in detail by a combination of experimental techniques and DFT computations. The adduct stability steadily decreases with increasing atomic number of the pnictine. The decreasing thermodynamic stability is accompanied by an increase of the X−Al−X bond angle (X = H, C) and a decrease of the Al−X bond lengths from the phosphine to the bismuthine adduct. The same structural trends were also found in the solid state by

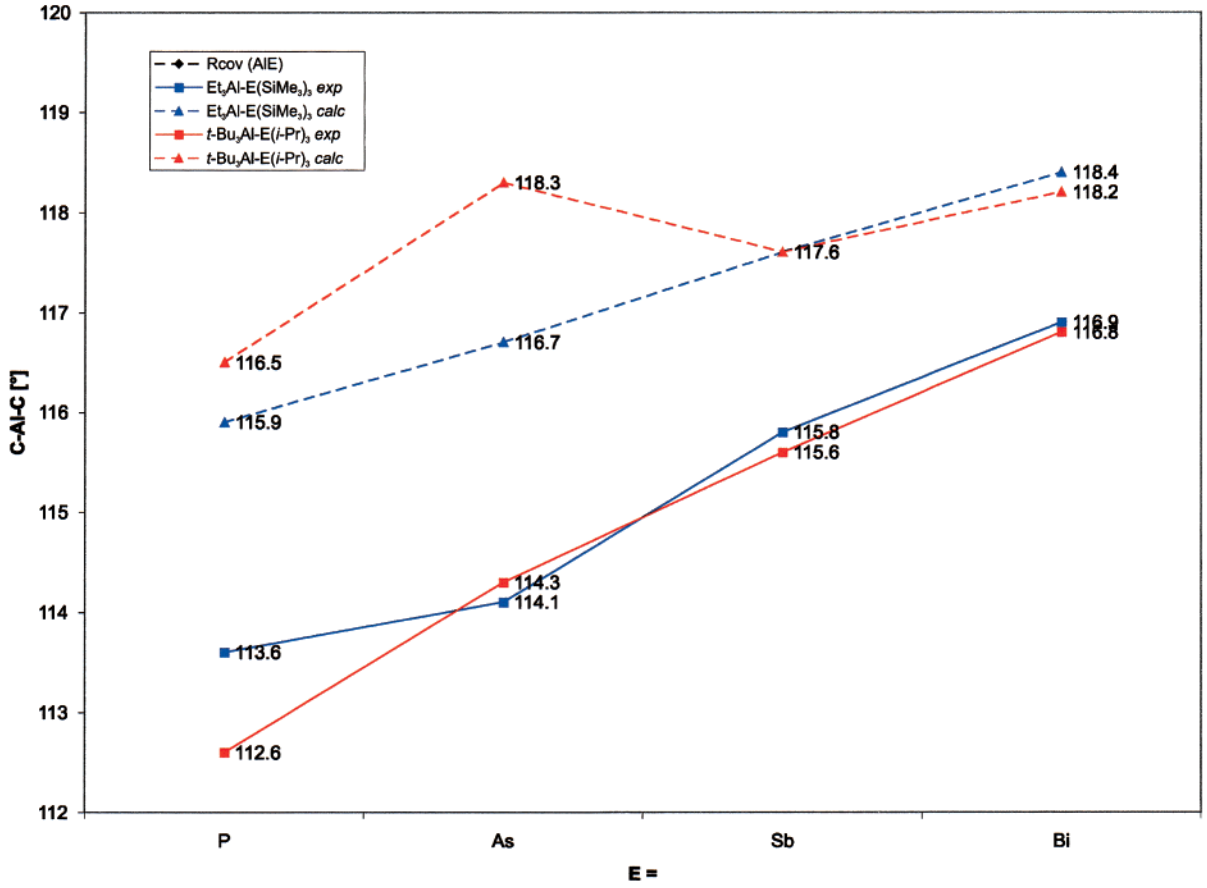

Figure 12. B3LYP/SDD optimized and experimental C−Al−C bond angles (deg) of $Et_3Al-E(SiMe_3)_3$ and t-$Bu_3Al-E(i$-$Pr)_3$ adducts.

single-crystal X-ray diffraction studies, which were performed for $Et_3Al-P(SiMe_3)_3$ and t-$Bu_3Al-E(i$-$Pr)_3$ adducts, showing the decreasing Lewis basicity of ER_3 with increasing atomic number of the pnictine. Temperature-dependent NMR spectroscopy studies on the t-$Bu_3Al-E(i$-$Pr)_3$ adducts also confirm this trend. The very bulky t-$Bu_3Al-E(i$-$Pr)_3$ adducts are difficult to describe computationally, due to pronounced repulsive van der Waals interactions, resulting in significantly decreased thermodynamic stabilities of the phosphine and arsine adducts. Such interactions are less dominant for the stibine and bismuthine adducts due to the increased atomic radii of the central pnictine.

Acknowledgment. S.S. and P.R.S. gratefully acknowledge generous financial support by the Deutsche Forschungsgemeinschaft (DFG) and the Fonds der Chemischen Industrie (FCI). S.S. thanks the Bundesministerium für Bildung, Wissenschaft, Forschung und Technologie (BMBF) and Prof. E. Niecke, Universität Bonn, for support. P.R.S. acknowledges support from the University of Georgia.

Supporting Information Available: Tables giving *xyz* coordinates and absolute energies of all computed species. This material is available free of charge via the Internet at http://pubs.acs.org.

OM0200205